

**M. Ociepa\*, M. Jenek, E. Feldshtein,  
K. Leksycki**

Institute of Machine Construction and Operations Engineering,  
University of Zielona Gora, Zielona Gora, Poland

\**m.ociepa@ibem.uz.zgora.pl*

## **The phenomenon of material side flow during finish turning of EN X153CrMoV12 hardened steel with tools based on polycrystalline cubic boron nitride**

*The study presents the results of an analysis of the phenomenon of material side flow during finish turning of EN X153CrMoV12 (H12MF GOST 5950-2000) tool steel hardened to  $63 \pm 2$  HRC with cutting tools made of polycrystalline composites based on polycrystalline cubic boron nitride. For an uncoated wedges of CBN 7025 the material side flow occurred for the entire range of tested cutting feed. For a CBN 8120 wedges with a TiAlN coating the side flow was observed exclusively for the cutting feed of  $f = 0.2$  mm/rev. The researched phenomenon did not occur on the surfaces finished with a CBN 7015 tool coated with TiN.*

**Keywords:** *polycrystalline cubic boron nitride, PCBN, hardened steel, finish turning, surface layer, material side flow.*

### **INTRODUCTION**

Finish turning of hardened materials differs significantly from processing of “soft” materials, mainly due to considerably greater hardness of the processed material ( $> 45$  HRC [1, 2], most commonly within 58–68 HRC [3]). Both the applied tool feed rates  $f$  and machining depth  $a_p$  are subject to significant restriction due to high cutting force [3, 4]. In contrast to machining of “soft” materials, machining of hardened ones is usually characterized by a negative rake angle which influences the compound cutting forces and causes high compressive stresses in the processed surface. Currently, hardened materials are machined without any cooling-lubricating liquids, which results in reaching temperatures of up to 1500 °C in the cutting zone [5]. That in turn can lead to damaging of surface layer and accelerating cutting tool wear.

Specific friction conditions which accompany the process of turning of hardened materials result in extremely high stresses in the cutting zone as well as plastic distortions of surface layer and the chip, often leading to a change in the structure of the processed material.

Processing of hardened materials is characterized by creation of the so called sawtooth chip [5–7], which creates a heat flux distribution different to the one obtained when turning “soft” materials. In this case, the friction of cutting surface against the processed material plays the major part while the plastic distortions and the friction of chip against rake face play a supporting role [5, 8].

Due to the process characteristics, the cutting wedges used in turning of hardened materials must display resistance to extensive mechanical load and higher

temperatures. Most commonly applied in machining of hardened materials is polycrystalline cubic boron nitride (PCBN). It is a material that displays high chemical stability event at temperatures exceeding 1400 °C, high impact strength and high resistance to thermal shock while being able to maintain its mechanical properties at high temperatures [9].

One of the effects of tribological disturbances in the cutting zone is the phenomenon of material side flow, firstly described in 1950 by Isaev in [10], which often occurs at finish turning. When occurring on the machined surface, this phenomenon is greatly undesirable as it may exert direct impact on deterioration of useful properties of surface layers [11, 12].

Material side flow leads to pushing the processed material in the direction opposite to direction of feed  $f$ . This is a direct effect of squeezing the material between the wedge surface and the machined surface which occurs right at the moment when the thickness  $h$  of the machined layer is smaller than the so called minimum thickness of machined layer  $h_{\min}$  (Fig. 1). The latter, on the other hand, depends on such factors as cutting feed  $f$  and cutting speed  $v_c$ , hardness and structure of machined material, as well as geometry of the cutting tool [13, 14, 15]. What is more, this phenomenon may as well be the effect of plasticized flow due to high temperatures and pressure which occur in the machining zone during hard turning of material by a worn cutting wedge, particularly in the event of notch wear [5, 11, 16]. Furthermore, according to Klimenko in [15] material side flow is caused by the collision of the two different material flows – first, removed by the major cutting edge, and second, removed by the minor cutting edges, which flows rates are different. The material flow traveling to the minor cutting edge is pushed to the side opposite to the feed  $f$  causing the material side flow.

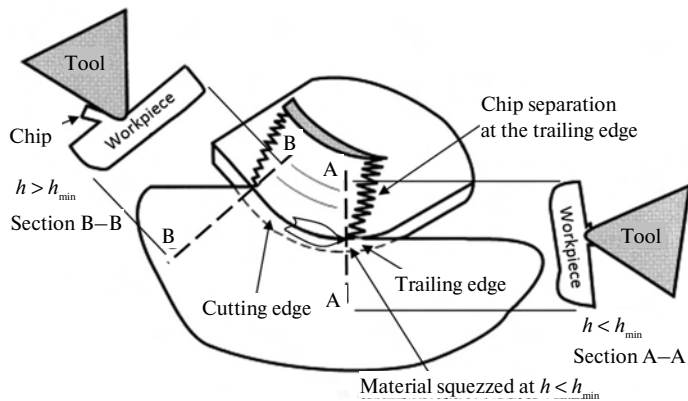


Fig. 1. The mechanism of material side flow in hard turning [5].

Suresh and Basavarajappa in [17] researched the wear of tools and condition of surface layer of AISI H13 (GOST 4ChPMF1S) tool steel hardened to 55 HRC under dry cutting with CVD-coated (TiC/TiCN/Al<sub>2</sub>O<sub>3</sub>) sintered carbide inserts at continuous and interrupted machining conditions with the parameters  $v_c = 80$ – $200$  m/min,  $a_p = 0.15$ – $0.75$  mm,  $f = 0.06$ – $0.26$  mm/rev. The increase in roughness of machined surface was related to wedge wear, which changed the geometry of cutting edge. This resulted in tribological disturbances in the cutting zone which led to the phenomenon of material side flow.

Kishawy and Elbestawi in [18] researched the condition of surface layer of AISI D2 (GOST H12MF) steel hardened to 62 HRC after HSC machining with PCBN tools. They demonstrated that surface roughness increased considerably

along with tool wear, mainly at cutting speeds above 350 m/min, which was attributed to material side flow. In the study [19] they also researched the influence of cutting parameters on the occurrence of that phenomenon during hard turning with PCBN tools. It was determined that material side flow was accompanied by high temperature at the cutting zone, which made the machined material behave as sticky liquid at the contact area of chip and tool.

The authors of study [16] found that the geometry of cutting edge directly influences the size and character of stagnation region from which material is removed due to side flow (Fig. 2). Along with the increase of the cutting wedge nose radius  $r_\epsilon$  and negative rake angle  $\gamma$  the stagnation region grows to the effect of intensifying of the phenomenon in question.

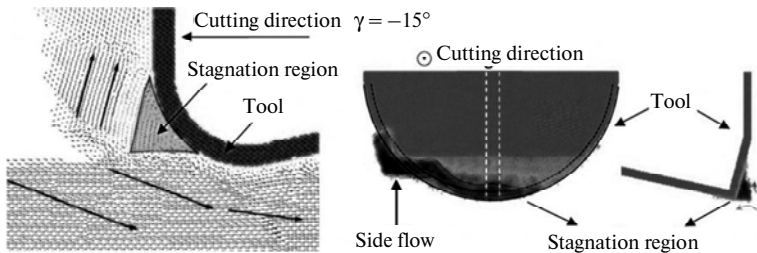


Fig. 2. The scheme presented creation of stagnation region and material side flow [14].

Coincident results can be found in the study [19] which analyzed the shaping of surface texture when turning of EN 41Cr4 (GOST 40H) hardened steel with PCBN cutting tools for machining parameters  $v_c = 165$  m/min,  $a_p = 0.2$  mm,  $f = 0.15$  mm/rev. Negative rake angle of the tools used during the research caused high cutting forces which resulted in high temperatures and pressure at the cutting zone. In turn that changed into material side flow which was distinguished by ridging of the workpieces and fraying of rough crests in the feed ridge area.

Zawada-Tomkiewicz in her study [20] analyzed the condition of surface layer of EN 41Cr4 steel hardened to 58 HRC machined with uncoated and TiN-coated PCBN tools of negative rake angle  $\gamma$ . Material side flow was determined for surfaces machined with both types of tool whereas it was more intense for uncoated wedge. That was explained by better tribological properties of the TiN-coated wedge in contact with the machined material.

The present research was aimed at comparative analysis of the impact of feed change  $f$  and of anti-wear coatings upon PCBN cutting wedges on the incidence of material side flow during finish turning of EN X153CrMoV12 (GOST H12MF) hardened steel.

## 2. RESEARCH CONDITIONS

In the research high-carbon high-chromium cold working EN X153CrMoV12 (GOST H12MF) tool steel was used whose chemical composition is presented in Table 1. The workpieces were hardened and then low tempered, which ensured hardness of  $63 \pm 2$  HRC.

**Table 1. Chemical composition of EN X153CrMoV12 (PN-EN ISO 4957:2002U) steel**

Chemical composition, wt %						
C	Si	Mn	Cr	Mo	V	Fe
1.45–1.6	0.1–0.6	0.2–0.6	11–13	0.7–1.0	0.7–1.0	the rest

Machining was performed for turning parameters:  $v_c = 160$  m/min,  $a_p = 0.2$  mm,  $f_1 = 0.1$  mm/rev,  $f_2 = 0.2$  mm/rev,  $f_3 = 0.3$  mm/rev. PDJNR2020K11 tool holder was used for the research, with replaceable inserts of DNGA 110408 type and the geometry  $\kappa_r = 93^\circ$ ,  $\alpha_0 = 6^\circ$ ,  $\gamma_0 = -6^\circ$ ,  $r_\epsilon = 0.8$  mm. The cutting wedge materials are presented in Table 2.

**Table 2. Material of cutting wedges used in the research**

Material grade	CBN 7025	CBN 7015	CBN 8120
Type of turning	continuous and light interrupted	continuous	continuous
PCBN structure	60 % CBN in ceramic bonding	50 % CBN in ceramic bonding	50 % CBN in ceramic bonding
Coating	none	TiN	TiAlN

Scanning microscope JEOL JSM-6400 was used for metallographic testing. The condition of machined surfaces was assessed with a three-axial optical gauging system Alicona Infinite SL combined with measurement software IF-Laboratory Measurement Module. The dry cutting conditions were used when turning.

### RESEARCH RESULTS

Condition of surfaces machined with uncoated CBN 7025 wedges is presented in Fig. 3. They demonstrate intense material side flow occurring on entire length of machined surfaces for all researched feed values  $f$ . There is a visible material flow in direction opposite to direction of feed  $f$ . The research phenomenon was observed to have been least intense for the highest feed  $f_3 = 0.3$  mm/rev.

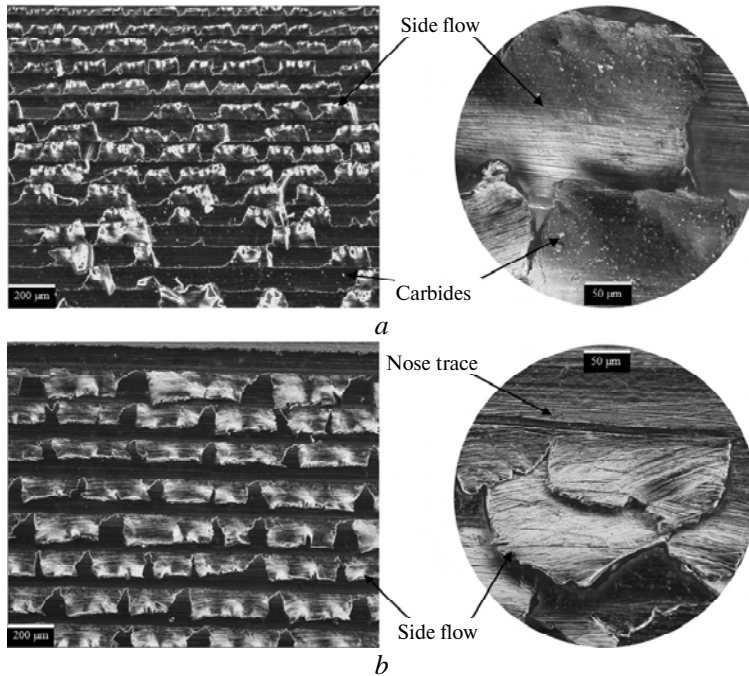


Fig. 3. Conditions of material surface after machining with uncoated CBN 7025 wedges for feed values  $f_1 = 0.1$  mm/rev (a),  $f_2 = 0.2$  mm/rev (b),  $f_3 = 0.3$  mm/rev (c).

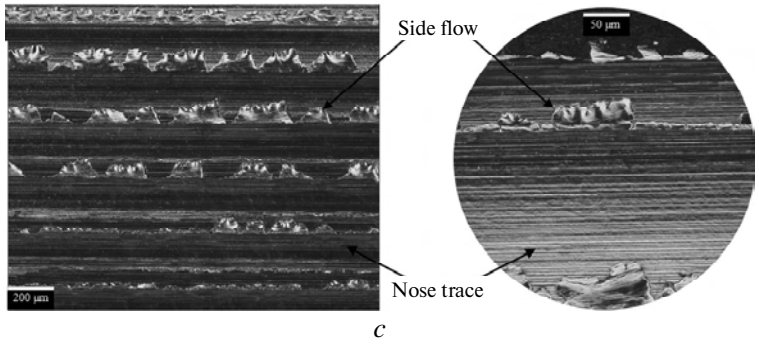


Fig. 3. (Contd.)

Figure 4 presents the condition of surfaces machined with TiAlN-coated CBN 8120 wedges. Material side flow was found exclusively for the surface turned at the feed of  $f_2 = 0.2$  mm/rev and it occurred along the entire length of machined surface.

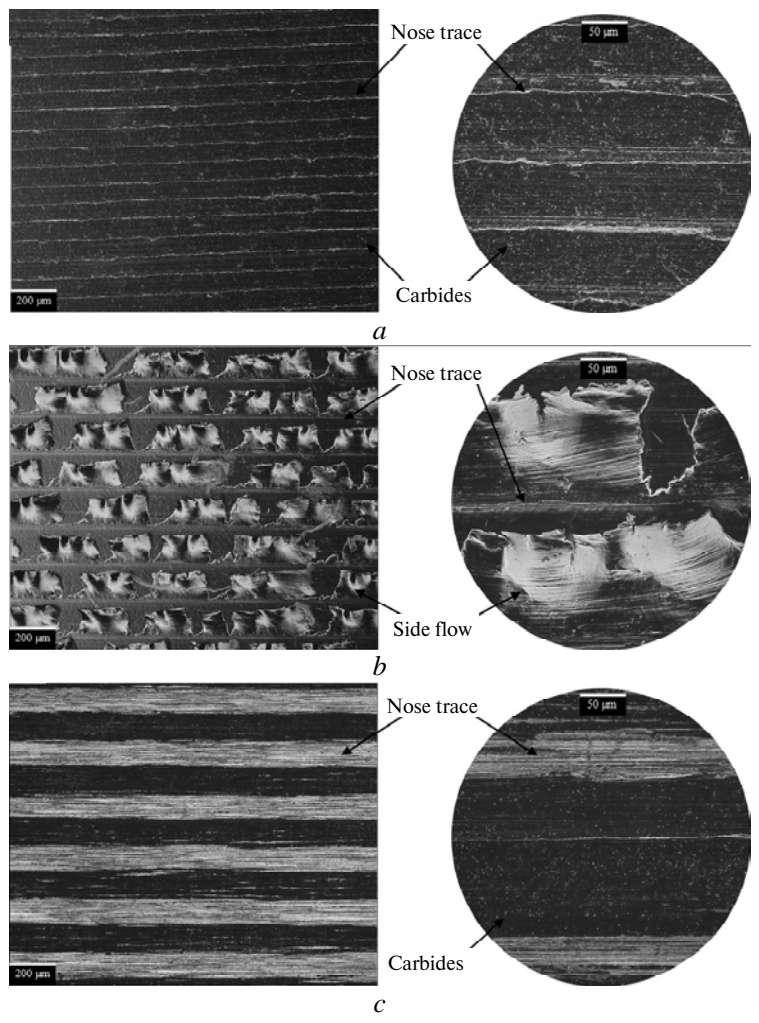


Fig. 4. Conditions of material surface after machining with TiAlN-coated CBN 8120 wedges for feed values  $f_{1n} = 0.1$  mm/rev (a);  $f_{2n} = 0.2$  mm/rev (b);  $f_{3n} = 0.3$  mm/rev (c).

Figure 5 presents the condition of surfaces machined with TiN-coated CBN 7015 wedges. No material side flow was found on the researched surfaces.

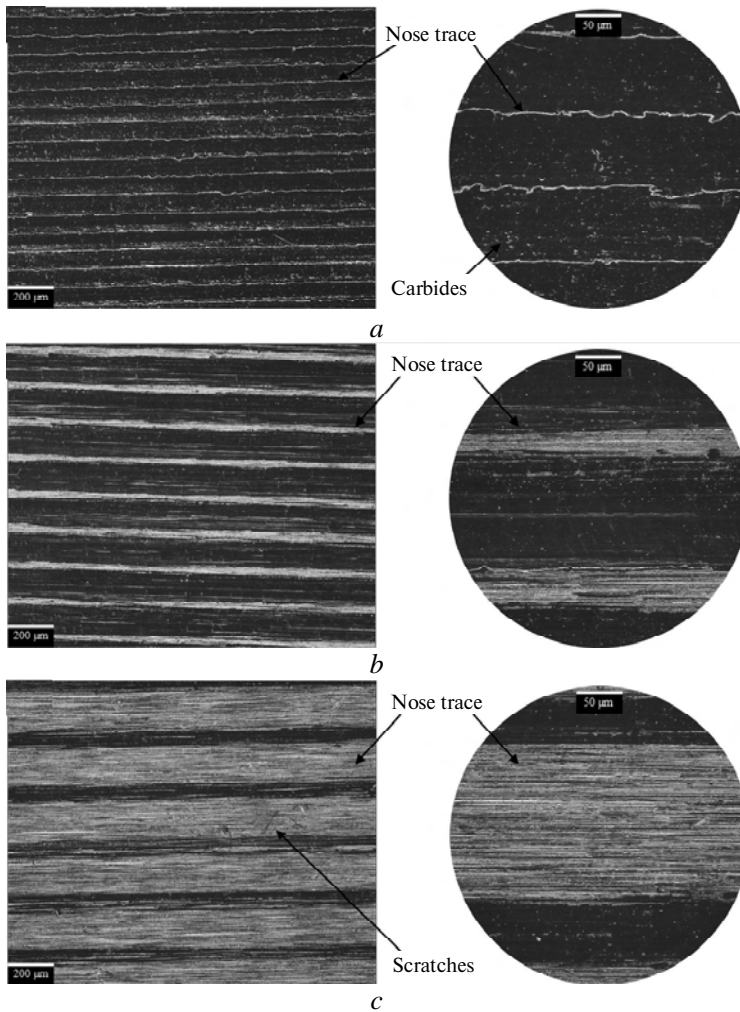


Fig. 5. Conditions of material surface after machining with TiN-coated CBN 7015 wedges for feed values  $f_1 = 0.1$  mm/rev (a);  $f_2 = 0.2$  mm/rev (b);  $f_3 = 0.3$  mm/rev (c).

Surfaces characterized with material side flow of the highest intensity, i.e. machined with CBN 7025 and CBN 8120 tools, both for feed value  $f_2 = 0.2$  mm/rev, tested with scanning microscope (Fig. 6).

In both cases there defects on the machined surface were visible in the form of side flow which was manifested as grooves and fraying of the machined material. For surfaces machined with the uncoated CBN 7025 wedge there were newly created cracks of significant size going deeply into the material, which might be the evidence of either extreme stresses or very high temperatures at the cutting zone. Furthermore, both surfaces demonstrated plastic deformations of the surface layer towards the feed direction  $f$ , sized 5–6  $\mu\text{m}$ , as well as distinct traces of the tool moving on the surface.

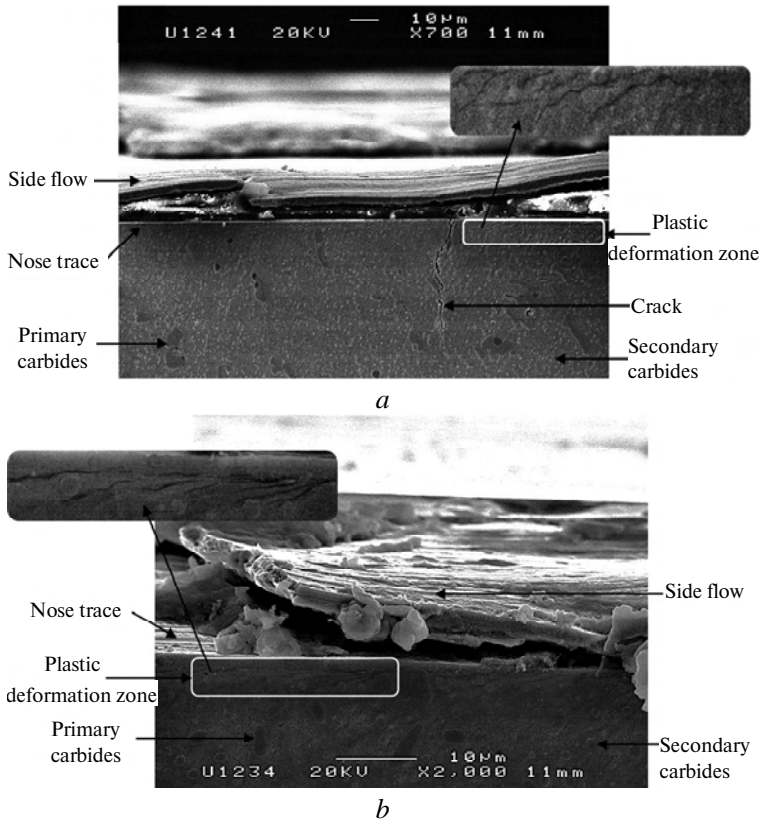


Fig. 6. Conditions of material surface after machining at feed value  $f_2 = 0.2$  mm/rev with uncoated CBN 7025 wedge (a) and TiAlN-coated CBN 8120 wedge (b).

## CONCLUSIONS

The study presents the results of an analysis of the phenomenon of material side flow during finish turning of EN X153CrMoV12 (H12MF GOST 5950-2000) tool steel hardened to  $63 \pm 2$  HRC with cutting tools made of polycrystalline composites based on PCBN. The research demonstrated varied intensity of the tested phenomenon, depending on the type of anti-wear coating applied on the wedges and the feed value. Absence of coating of the wedges resulted in intense material side flow for the entire tested feed range  $f = 0.1-0.3$  mm/rev. Surfaces machined with TiN-coated wedges did not show any traces of material side flow in the entire range of feed values. For surfaces machined with TiAlN-coated wedges, material side flow was manifested only for the feed value  $f = 0.2$  mm/rev. SEM analysis of the material side flow areas demonstrated defects in the surface layer, namely a distinct  $5-6 \mu\text{m}$  thick zone of plastic deformations. Furthermore, the structure of the material machined with uncoated wedges displayed cracks perpendicular to the machined surface, caused by extreme residual machining stress in the surface layer and high temperatures in the cutting zone.

*Представлено результати аналізу феномену бічного нагромадження матеріалу після чистової токарної обробки інструментальної сталі EN X153CrMoV12 (H12MF ГОСТ 5950-2000), загартованої до  $63 \pm 2$  HRC, при використанні ріжучих інструментів з полікристалічних композитів на основі полікристалічного кубічного нітриду бору. Для непокритих вставок з CBN 7025 бічне нагромадження матеріалу відбувалося для всього випробуваного діапазону подачі при різанні. Для вставок з CBN 8120 з покрит-*

тям TiAlN бічне нагромадження спостерігали виключно для подачі при різанні  $f = 0,2$  мм/об. Досліджуваний феномен не відбувався на поверхнях, оброблених інструментом CBN 7015, покритим TiN.

**Ключові слова:** полікристалічний кубічний нітрид бору, PCBN, загартована сталь, фінішне обточування, поверхневий шар, бічне нагромадження матеріалу.

Представлены результаты анализа феномена бокового нагромаждения материала после чистовой токарной обработки инструментальной стали EN X153CrMoV12 (H12MF ГОСТ 5950-2000), закаленной до  $63 \pm 2$  HRC, с помощью режущих инструментов из поликристаллических композитов на основе поликристаллического кубического нитрида бора. Для непокрытых вставок из CBN 7025 боковое нагромаждение материала происходило для всего исследованного диапазона подачи при резании. Для вставок из CBN 8120 с покрытием TiAlN боковое нагромаждение наблюдали исключительно для подачи при резании  $f = 0,2$  мм/об. Исследованное явление не происходило на поверхностях, обработанных инструментом CBN 7015, покрытым TiN.

**Ключевые слова:** поликристаллический кубический нитрид бора, PCBN, закаленная сталь, чистовая токарная обработка, поверхностный слой, боковое нагромаждение материала.

1. Kumar R., Kumar Sahoo A., Kumar Das R., Panda A., Chandra Mishra P. Modelling of flank wear, Surface roughness and cutting temperature in sustainable hard turning of AISI D2 steel. *Proc. Manufact.* 2018. Vol. 20. P. 406–413.
2. Srithar A., Palanikumar K., Durgaprasad B. Experimental investigation and surface roughness analysis on hard turning of AISI D2 steel using coated carbide insert. *Proc. Eng.* 2014. Vol. 97. P. 72–77.
3. Gong F., Zhao J., Pang J. Evolution of cutting forces and tool failure mechanisms in intermittent turning of hardened steel with ceramic tool. *Int. J. Adv. Manufact. Technol.* 2017. Vol. 89(5–8). P. 1603–1613.
4. Pal A., Choudhury S.K., Chinchankar S. Machinability assessment through experimental investigation during hard and soft turning of hardened steel. *Proc. Mater. Sci.* 2014. Vol. 6. P. 80–91.
5. Grzesik W. Mechanics of cutting and chip formation. *Machining of Hard Materials*. London: Springer-Verlag, 2011. P. 87–114.
6. Tang L., Yin J., Sun Y., Shen H., Gao C. Chip formation mechanism in dry high-speed orthogonal turning of hardened AISI D2 tool steel with different hardness levels. *Int. J. Adv. Manufact. Technol.* 2017. Vol. 93. P. 2341–2356.
7. Jomaa W., Ben Fredj N., Zaghbani I., Songmene V. Non-conventional turning of hardened AISI D2 tool steel. *Int. J. Adv. Machin. Form. Opera.* 2011. Vol. 3(2). P. 93–126.
8. Chen L., Tai B.L., Chaudhari R.G., Song X., Shih A.J. Machined Surface temperature in hard turning. *Int. J. Mach. Tools Manufact.* 2017. Vol. 121. P. 10–21.
9. Tillmann W., Elrefaey A., Wojarski L. Brazing of cutting tools. *Adv. Brazing – Sci., Technol., Appl.* 2013. P. 423–471.
10. Isaev A.I. The Mechanism of Formation of Surface Layer During Metal Cutting [in Russian]. Moscow: Mashgiz, 1950.
11. Suresh R., Basavarajappa S., Gaitonde V.N., Samuel G.L., Davim J.P. State-of-the-art research in machinability of hardened steels. *J. Eng. Manufact.* 2013. Vol. 227, no. 2. P. 191–209.
12. Zawada-Tomkiewicz A. Analysis of surface roughness parameters achieved by hard turning with the use of PCBN tools. *Estonian J. Eng.* 2011. Vol. 17, no. 1. P. 88–99.
13. Coelho R.T., Diniz A.E., de Silva T.M. An experimental method to determine the minimum uncut chip thickness ( $h_{min}$ ) in orthogonal cutting. *Proc. Manufact.* 2017. Vol. 10. P. 194–207.
14. Schultheiss F., Hagglund S., Bushlya V., Zhou J., Stahl J.E. Influence of the minimum chip thickness on the obtained Surface roughness during turning operations. *Proc. CIRP.* 2014. Vol. 13. P. 67–71.
15. Klimenko S.A. On the mechanism of the surface microgeometry formation in cutting. *J. Superhard Mater.* 1997. Vol. 19, no. 5. P. 43–53.
16. Xu F., Fang F., Zhang X. Side flow effect on surface generation in nano cutting. *Nanoscale Res. Lett.* 2017. Vol. 12, no. 1, art. 359.



17. Suresh R., Basavarajappa S. Turning of hardened H13 steel with interrupted and continuous surfaces using multilayer coated carbide tool. *5th Int. & 26th All India Manufact. Technol., Design Res. Conf. AIMTDR 2014*. 2014. December, art. 25.
18. Kishawy H.A., Elbestawi M.A. Tool wear and surface integrity during high speed turning of hardened steel with PCBN tools. *Proc. Inst. Mech. Eng., Part B: J. Eng. Manufact.* 2001. Vol. 215, no. 6. P. 755–767.
19. Kishawy H.A., Elbestawi M.A. Effect of process parameters on material side flow during hard turning. *Int. J. Machine Tools Manufact.* 1999. Vol. 39, no. 7. P. 1017–1030.
20. Zawada-Tomkiewicz A. Analiza kształtowania struktury geometrycznej powierzchni w mikroskali dla procesu toczenia stali utwardzonej. *Mechanik*. 2015. Vol. 8–9. P. 19–27.

Received 15.11.18

Revised 31.01.19

Accepted 13.02.19